4648 *Inorg. Chem.* **2010**, *49*, 4648–4656
DOI: 10.1021/ic1004193

Inorganic Chemistry
Article

# (dme)$MCl_3(NNPh_2)$ (dme = dimethoxyethane; M = Nb, Ta): A Versatile Synthon for [Ta=$NNPh_2$] Hydrazido(2-) Complexes†

**Ian A. Tonks and John E. Bercaw***

*Arnold and Mabel Beckman Laboratories of Chemical Synthesis, California Institute of Technology, Pasadena, California 91125*

Received March 2, 2010

Complexes (dme)$TaCl_3(NNPh_2)$ (**1**) and (dme)$NbCl_3(NNPh_2)$ (**2**) (dme =1,2-dimethoxyethane) were synthesized from $MCl_5$ and diphenylhydrazine via a Lewis-acid assisted dehydrohalogenation reaction. Monomeric **1** has been characterized by X-ray, IR, UV−vis, $^1$H NMR, and $^{13}$C NMR spectroscopy and contains a $\kappa^1$-bound hydrazido(2-) moiety. Unlike the corresponding imido derivatives, **1** is dark blue because of an LMCT that has been lowered in energy as a result of an $N_\alpha-N_\beta$ antibonding interaction that raises the highest occupied molecular orbital (HOMO). Reaction of **1** with a variety of neutral, mono- and dianionic ligands generates the corresponding ligated complexes retaining the $\kappa^1$-bound [Ta−$NNPh_2$] moiety.

## Introduction

A longstanding goal in chemistry is the activation and subsequent functionalization of molecular dinitrogen.[1] One of the proposed intermediates along a Chatt-type[2] cycle of $N_2$ reduction is an end-on ($\kappa^1$-) bound hydrazide (2-) moiety ($M=NNH_2$), and accordingly significant research into possible models for these intermediates based on group 5−8 metals has been undertaken.[3] In addition to efforts toward the synthesis of ammonia from dinitrogen, recent work toward the synthesis of other nitrogen-containing products from [$M=NNR_2$] moieties has proven to be an active area of investigation. Following Bergman's first report,[4] the groups of Mountford,[5] Odom,[6] and Gade[7] have been exploring the reactivity of group 4 hydrazides and have made significant advances in the implementation of these complexes in catalytic nitrene transfer[8] and hydrohydrazination reactions. Additionally, Fryzuk and co-workers have reported an interesting dinuclear tantalum complex with a bridging, side-on, end-on bound $N_2$ ligand that could be also considered a formal hydrazido moiety. This complex is particularly susceptible to N−N bond cleavage and further functionalization to afford silylamines.[9]

While there exist examples of end-on ($\kappa^1$-) hydrazide (2-) vanadium complexes,[3a,10] few complexes of the heavier congeners Nb[11] and Ta[12] have been synthesized and

† Dedicated to Professor Uwe Rosenthal on the occasion of his 60th birthday.

*To whom correspondence should be addressed. E-mail: bercaw@caltech.edu.

(1) (a) Fryzuk, M. D.; Johnson, S. A. *Coord. Chem. Rev.* **2000**, *200*, 379. (b) MacKay, B. A.; Fryzuk, M. D. *Chem. Rev* **2004**, *104*, 385.

(2) Chatt, J.; Dilworth, J. R.; Richards, R. L. *Chem. Rev.* **1978**, *78*, 589.

(3) For representative examples, see: (a) Banerjee, S.; Odom, A. L. *Dalton Trans.* **2008**, 2005. (b) Yandulov, D. V.; Schrock, R. R. *Science* **2003**, *301*, 76. (c) Schrock, R. R.; Glassman, T. E.; Vale, M. G.; Kol, M. *J. Am. Chem. Soc.* **1993**, *115*, 1760. (d) Dilworth, J. P.; Jobanputra, P.; Parrott, S. J.; Thompson, R. M.; Povey, D. C.; Zubieta, J. A. *Polyhedron* **1992**, *11*, 147. (e) Huynh, M. H. V.; Lee, D. G.; White, P. S.; Meyer, T. J. *Inorg. Chem.* **2001**, *40*, 3842. (f) Huynh, M. H. V.; El-Samanody, E. S.; Demadis, K. D.; White, P. S.; Meyer, T. J. *Inorg. Chem.* **2000**, *39*, 3075. (g) Coia, G M.; Devenney, M.; White, P. S.; Meyer, T. J. *Inorg. Chem.* **1997**, *36*, 2341.

(4) Walsh, P. J.; Carney, M. J.; Bergman, R. G. *J. Am. Chem. Soc.* **1991**, *113*, 6343.

(5) (a) Parsons, T. B.; Hazari, N.; Cowley, A. R.; Green, J. C.; Mountford, P. *Inorg. Chem.* **2005**, *44*, 8442. (b) Selby, J. D.; Manley, C. D.; Feliz, M.; Schwarz, A. D.; Clot, E.; Mountford, P. *J. Chem. Soc., Chem. Commun.* **2007**, 4937. (c) Selby, J. D.; Schulten, C.; Schwarz, A. D.; Stasch, A.; Clot, E.; Jones, C.; Mountford, P. *J. Chem. Soc., Chem. Commun.* **2008**, 5101. (d) Clulow, A. J.; Selby, J. D.; Cushion, M. G.; Schwarz, A. D.; Mountford, P. *Inorg. Chem.* **2008**, *47*, 12049. (e) Selby, J. D.; Manley, C. D.; Schwarz, A. D.; Clot, E.; Mountford, P. *Organometallics* **2008**, *27*, 6479.

(6) (a) Li, Y.; Shi, Y.; Odom, A. L. *J. Am. Chem. Soc.* **2004**, *126*, 1794. (b) Patel, S.; Li, Y.; Odom, A. L. *Inorg. Chem.* **2007**, *46*, 6373.

(7) (a) Herrmann, H.; Fillol, J. L.; Wadepohl, H.; Gade, L. H. *Angew. Chem., Int. Ed.* **2007**, *46*, 8426. (b) Herrmann, H.; Fillol, J. L.; Gehrmann, T.; Enders, M.; Wadepohl, H.; Gade, L. H. *Chem.—Eur. J.* **2008**, *14*, 8131. (c) Herrmann, H.; Wadepohl, H.; Gade, L. H. *J. Chem. Soc., Dalton Trans.* **2008**, 2111. (d) Herrman, H.; Gehrmann, T.; Wadepohl, H.; Gade, L. H. *J. Chem. Soc., Dalton Trans.* **2008**, 6231. (e) Weitershaus, K.; Wadepohl, H.; Gade, L. H. *Organometallics* **2009**, *28*, 3381. (f) Weitershaus, K.; Fillol, J. L.; Wadepohl, H.; Gade, L. H. *Organometallics* **2009**, *28*, 4747.

(8) Mindiola, D. J. *Angew. Chem., Int. Ed.* **2008**, *47*, 2.

(9) (a) Fryzuk, M. D. *Acc. Chem. Res.* **2009**, *42*, 127. (b) Shaver, M. P.; Fryzuk, M. D. *J. Am. Chem. Soc.* **2005**, *127*, 500. (c) MacKay, B. A.; Munha, R. F.; Fryzuk, M. D. *J. Am. Chem. Soc.* **2006**, *128*, 9472.

(10) (a) Davies, S. C.; Hughes, D. L.; Janas, Z.; Jerzykiewicz, L.; Richards, R. L.; Sanders, J. R.; Sobota, P. *Chem. Commun.* **1997**, 1261. (b) Henderson, R. A.; Janas, Z.; Jerzykiewicz, L. B.; Richards, R. L.; Sobota, P. *Inorg. Chim. Acta* **1999**, *285*, 178. (c) Davies, S. C.; Hughes, D. L.; Janas, Z.; Jerzykiewicz, L.; Richards, R. L.; Sanders, J. R.; Silverston, J. E.; Sobota, P. *Inorg. Chem.* **2000**, *39*, 3485. (d) Davies, S. C.; Hughes, D. L.; Konkol, M.; Richards, R. L.; Sanders, J. R.; Sobota, P. *J. Chem. Soc., Dalton Trans.* **2002**, 2811.

(11) Green, M. L. H.; James, J. T.; Saunders, J. F.; Souter, J. *J. Chem. Soc., Dalton Trans.* **1997**, 1281.

(12) Sebe, E.; Heeg, M. J.; Winter, C. H. *Polyhedron* **2006**, *25*, 2109.


Published on Web 04/19/2010

characterized. In fact, only two related complexes containing [Ta═$NNR_2$] have been reported: [Ta($NNR_2$)$Cl_2$($NH_2NR_2$)-(TMEDA)]Cl (R = Me, 1,5-$(CH_2)_5$).[12] The utilization of these complexes to prepare other related hydrazido complexes appears limited—all attempts to replace the chloride ligands with amides or alkoxides through salt metathesis reactions have failed. The methodology used to prepare [V = $NNR_2$] complexes, aminolysis of vanadium oxo[10c] or phenoxide[10b] ligands, is not viable for niobium and tantalum because of their increased oxophilicity. Additionally, this methodology typically requires installing the ancillary ligand scaffold before the [M = $NNR_2$] moiety. With this in mind, we sought to develop a simple synthetic entry point into niobium and tantalum terminal [M = $NNR_2$] complexes and investigate their reactivity relative to analogous tantalum imido complexes and also to group 4 [M = $NNR_2$] moieties. Herein we report the synthesis of a versatile group 5 end-on ($\kappa^1$-) hydrazido synthon, (dme)M($NNPh_2$)$Cl_3$ (dme = $CH_3$-$OCH_2CH_2OCH_3$; M = Nb, Ta), along with initial results for the tantalum complex demonstrating that dme and chloride may be cleanly displaced by a variety of chelating ligands.

## Results and Discussion

Following a procedure similar to those utilized by Williams et al. to prepare group 5 [Ta═NR] imido complexes,[13] $TaCl_5$ and $NbCl_5$ were treated with diphenylhydrazine and dimethoxyethane (dme) in the presence of pyridine and $ZnCl_2$ to generate (dme)$TaCl_3$($NNPh_2$) (**1**) and (dme)$NbCl_3$($NNPh_2$) (**2**), respectively, through a Lewis acid assisted dehydrohalogenation reaction (eq 1).[14] Unfortunately, similar reactions involving $Me_2NNH_2$, $MePhNNH_2$, or N-aminopiperidine yield intractable mixtures of products, possibly a result of the increased basicity of the $N_\beta$ lone pair and/or the better bridging ability of these less bulky hydrazines. The dme ligand in **1** and **2** exhibits two signals in the $^1$H and $^{13}$C NMR spectra for the methoxy protons, as well as two signals for the methylene protons, indicating a *cis*, *mer* geometry as indicated in eq 1.

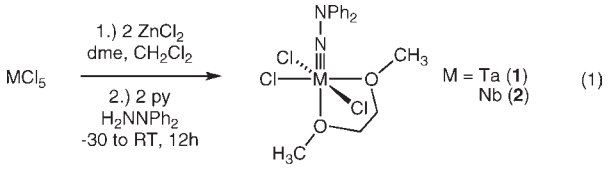


**1** was crystallized by vapor diffusion of pentane into a concentrated 1,2-dichloroethane solution of **1** to give large, blue needles. The X-ray structure of **1** (Figure 1) confirms that the complex is monomeric containing an end-on, $\kappa^1$-bound diphenylhydrazido(2-) ligand. In agreement with NMR data, the ligands are arranged in a *cis,mer* fashion, with one of the dme oxygens *trans* to a chloride and the other *trans* to the hydrazide ligand. The Ta−N1 bond distance in **1** is 1.773(1) Å which indicates a Ta−N $LX_2$ triple bond, as does the nearly linear Ta−N1−N2 bond angle (173.65(8)°).

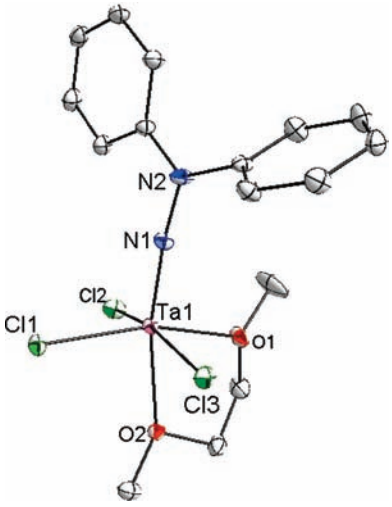


**Figure 1.** Thermal ellipsoid drawing of **1**. Selected bond lengths (Å) and angles (deg): Ta1−N1 1.773(1); Ta1−O1 2.1638(7); Ta1−O2 2.2953(9); N1−N2 1.347(1); Ta1−N1−N2 173.65(8). H atoms removed for clarity.

The N1−N2 distance of 1.347(1) is slightly shorter than that of free diphenylhydrazine, which would be expected on the basis of reduced $N_\alpha-N_\beta$ lone pair repulsion resulting from $N_\alpha$ lone pair donation to the metal center.

In some $MNNR_2$ complexes it is possible that the hydrazide unit could be described as a formally neutral diazene L-type ligand,[15] but the short Ta−N distance, the only slightly shortened $N_\alpha-N_\beta$ bond, and nearly linear Ta−$N_\alpha-N_\beta$ bond angle indicate that the $LX_2$-type hydrazido(2-) resonance structure is the major contributor in **1**.

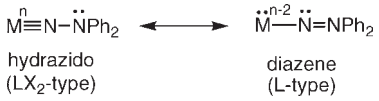


A particularly interesting characteristic of **1** is its unique dark blue color. UV−vis studies of **1** show a prominent ligand-to-metal charge transfer (LMCT) band at 583 nm with an extinction coefficient of 400 $M^{-1}$ $cm^{-1}$. In contrast, the corresponding imido complexes (dme)$TaCl_3$($N^tBu$) and (dme)$TaCl_3$(NPh) are colorless (342 nm) and pale yellow (425 nm), respectively.[13] The LMCT in these imido complexes is postulated to arise from a transition from Ta $d_{xz}$−$N_\alpha$ $p_x$ $\pi$ bonding orbital (HOMO) to the unoccupied Ta $d_{xy}$ orbital (LUMO).[16] We attribute the large red shift in the LMCT for **1** to the interaction of the $N_\beta$ lone pair with the Ta $d_{xz}-N_\alpha$ $p_x$ $\pi$ bonding orbital that serves to destabilize the HOMO via an $N_\alpha-N_\beta$ antibonding interaction (Scheme 1).

A similar phenomenon is observed in (dme)$TaCl_3$(NPh) as a result of an antibonding contribution from the aryl ring, although the effect is smaller (Scheme 1).[17] DFT calculations (see Experimental Section for computational details) of the HOMO−LUMO gap performed on **1**, (dme)$TaCl_3$($NCMe_3$), and (dme)$TaCl_3$(NPh) qualitatively agree with this assessment, and the $N_\alpha-N_\beta$ and $N_\alpha$−phenyl $\pi$ antibonding interactions for the HOMOs are clearly evident in **1** and

(13) Korolev, A. V.; Rheingold, A. L.; Williams, D. S. *Inorg. Chem.* **1997**, *36*, 2647.

(14) In all of the schemes in this paper, amido (LX) ligands will be represented as double bonds and imido ligands ($LX_2$) as triple bonds since these representations most accurately describe the bonding within these systems (as evidenced by simple electron counting and DFT calculations), despite this notation not being the normal convention.

(15) Danopoulos, A. A.; Hay-Motherwell, R. S.; Wilkinson, G.; Sweet, T. K. N.; Hursthouse, M. B. *Polyhedron* **1997**, *16*, 1081.

(16) Williams, D. S.; Thompson, D. W.; Korolev, A. V. *J. Am. Chem. Soc.* **1996**, *118*, 6526.

(17) Williams, D. S.; Korolev, A. V. *Inorg. Chem.* **1998**, *37*, 3809.

**Scheme 1**

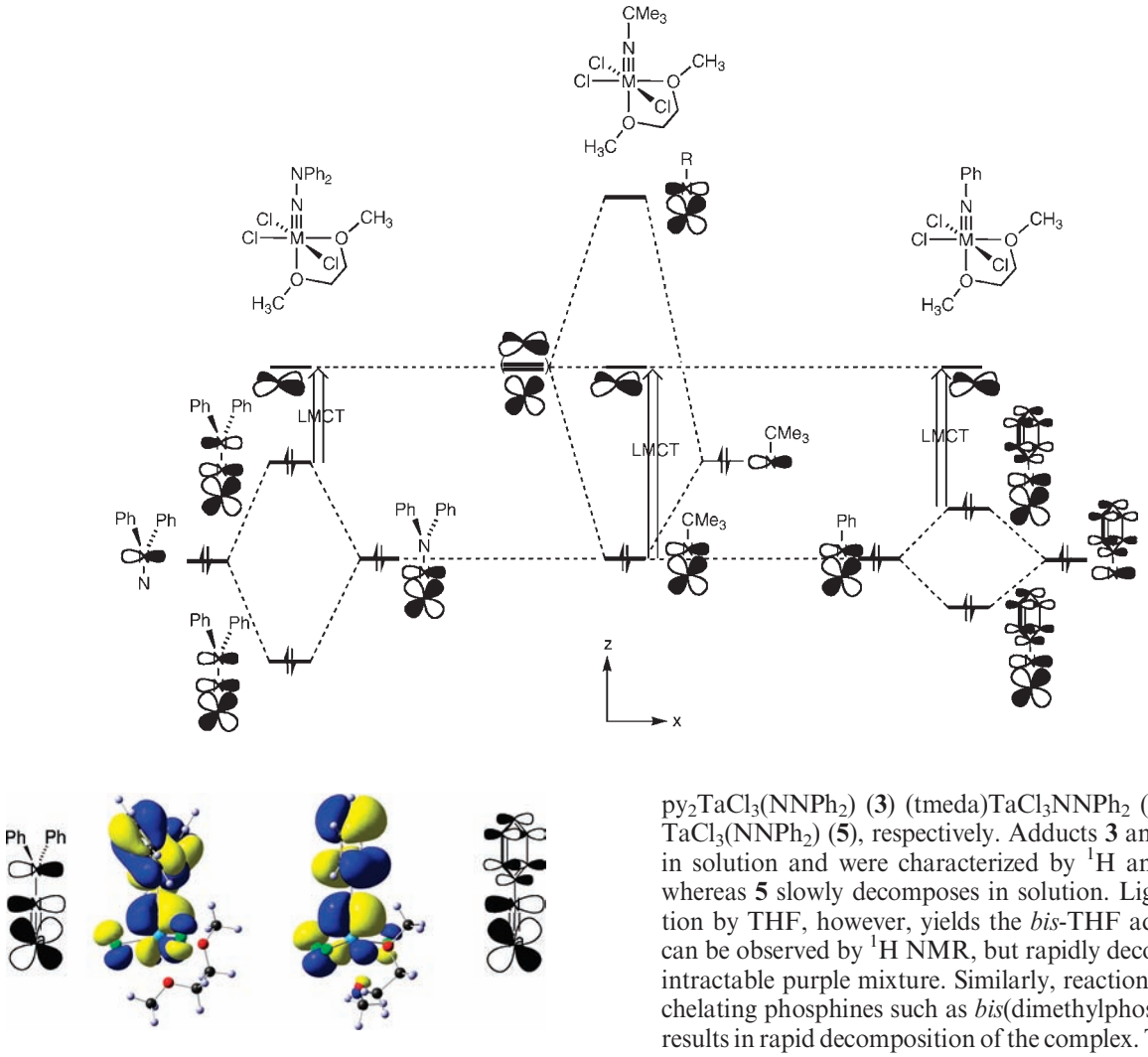


**Figure 2.** Schematic of HOMOs derived from DFT calculations performed on (dme)$TaCl_3(NNPh_2)$ (**1**) (left) and (dme)$TaCl_3$(NPh) (right) showing antibonding interactions between the Ta−N $\pi$ bond and $N_\beta$ and phenyl substituents, respectively.

(dme)$TaCl_3$(NPh) (Figure 2).[18] The calculated HOMO−LUMO gaps for all three compounds were consistently larger than the observed values, so that quantitative comparisons on the lone pair and aryl $\pi$ effects are not possible. One particularly enticing aspect of this effect is that the addition of a -lone pair destabilizes the M = N multiple bond, which could increase the reactivity of hydrazido(2-) complexes toward [2 + 2] cyclization reactions as compared to the parent imidos.

**1** undergoes ligand substitution with a variety of neutral L-donors to generate new complexes bearing a terminal diphenylhydrazido(2-) moiety (eq 2). The dme ligand is readily substituted by nitrogen based L donors: pyridine, tmeda, and bipyridine will react with **1** in benzene to yield $py_2TaCl_3(NNPh_2)$ (**3**) (tmeda)$TaCl_3NNPh_2$ (**4**) and (bpy)-$TaCl_3(NNPh_2)$ (**5**), respectively. Adducts **3** and **4** are stable in solution and were characterized by $^1$H and $^{13}$C NMR, whereas **5** slowly decomposes in solution. Ligand substitution by THF, however, yields the *bis*-THF adduct **6** which can be observed by $^1$H NMR, but rapidly decomposes to an intractable purple mixture. Similarly, reaction with $PPh_3$ or chelating phosphines such as *bis*(dimethylphosphino)ethane results in rapid decomposition of the complex. The instability of these complexes likely is a result of weaker monodentate ether or softer phosphine donors.

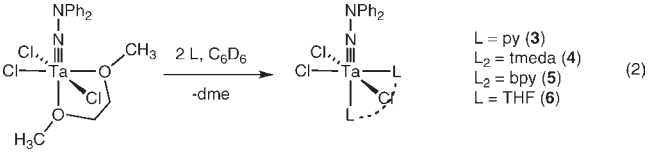


Precursor **1** also reacts cleanly with a variety of mono- and dianionic ligands. Treatment of **1** with 2 equiv of NaCp generates the tantalocene product $Cp_2TaCl(NNPh_2)$ (**7**) in good yield (eq 3). Treatment of **1** with only 1 equiv of NaCp gives 0.5 equiv of **7** and 0.5 equiv of **1**, and thus far we have been unable to prepare monocyclopentadienyl complexes of the type $CpTaCl_2(NNR_2)$ via **1**. Orange crystals of **7** were obtained by layering pentane onto a concentrated toluene solution cooled to −30 °C. The X-ray structure of **7** is reported in Figure 3. The bonding in **7** is different from all other [Ta=NNR$_2$] complexes reported here. Since the vacant orbital on Ta perpendicular to the tantalocene equatorial plane that is capable of forming a second Ta−N $\pi$ bond is Ta−Cp antibonding,[19] **7** should have a weaker Ta≡N triple

(18) One reviewer pointed out that in the $NNPh_2$ case, in addition to the lone pair effect, delocalization into the aryl rings may play an important role in the HOMO. Our DFT calculations show that there appears to be contribution from the aryl $\pi$ system. This is further supported by some related tungsten complexes, where the diphenylhydrazidos have a very low energy LMCT when compared to the dialkylhydrazidos; see: Koller, J.; Ajmera, H. M.; Abboud, K. A.; Anderson, T. J.; McElwee-White, L. *Inorg. Chem.* **2008**, *47*, 4457. We are currently investigating this effect as it relates to other heteroatom substituted imido derivatives.

(19) Parkin, G.; van Asselt, A.; Leahy, D. J.; Whinnery, L.; Hua, N. G.; Quan, R. W.; Henling, L. M.; Schaefer, W. P.; Santarsiero, B. D.; Bercaw, J. E. *Inorg. Chem.* **1992**, *31*, 82.

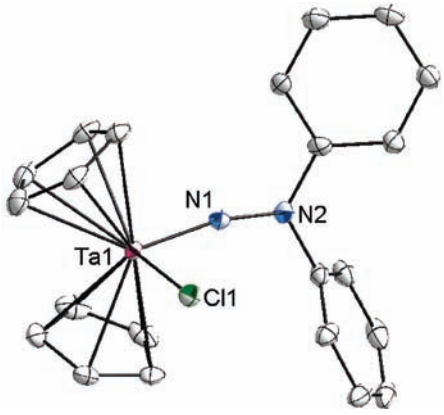


**Figure 3.** Thermal ellipsoid drawing of **7**. Selected bond lengths (Å) and angles (deg): Ta1−N1 1.8153(16); N1−N2 1.3358(22); Ta1−N1−N2 167.04(1). Summation of angles about N2: 358°. H atoms removed for clarity.

bond, approaching more of Ta═N double bond. This intermediate bond order is reflected in the Ta−N bond distance, which at 1.8153(16)Å is longer than all other Ta−N triple bonds which are reported here. Because of the low symmetry of this molecule, it is difficult to determine the occupation of the Ta−Cp antibonding orbital based on Ta−C bond lengths. The Ta−$N_\alpha$−$N_\beta$ bond angle is bent out of the tantalocene wedge to 167.04(1)°, which might also be indicative of some Ta═N character with a stereochemically active $N_\alpha$ lone electron pair as shown in eq 3, but this distortion from linearity might be due at least in part to steric interactions between cyclopentadienyl ligands and the large [$N_\beta Ph_2$] group (closest non-bonded H−H contacts between the [$N_\beta Ph_2$] group and the Cp ring are 2.263 and2.426 Å). Again, the low symmetry makes distinguishing between electronic and steric effects difficult.

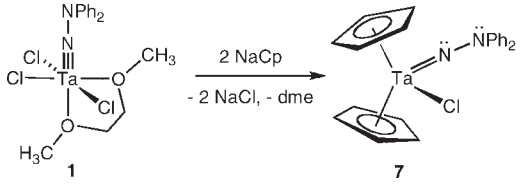


(3)

Recently, our group has been interested in using aryl-linked *bis*(phenolate) ligand sets as analogues of *bis*(cyclopentadienyl) scaffolds.[20] Hydrazide-containing tantalum *bis*(phenolate) complexes have been synthesized through two methods. First, the salt metathesis reaction of **1** with (2,6-(OC$_6$H$_2$-$^t$Bu$_2$)$_2$C$_5$H$_3$N)K$_2$ in benzene in the presence of excess pyridine led to quantitative formation (NMR) of (ONO)TaCl(NNPh$_2$)(py) (**8**) (ONO = (2,6-(OC$_6$H$_2$-$^t$Bu$_2$)$_2$-C$_5$H$_3$N)) (eq 4). The addition of a sixth ligand (e.g., pyridine) to these reactions is required: attempts to synthesize the related 5-coordinate complexes without an additional L donor always yielded intractable, insoluble product mixtures. Alternately, the complex (ONO)TaCl(NNMe$_2$)(HNMe$_2$) (**9**) could be synthesized through hydrazinolysis of (ONO)Ta(NMe$_2$)$_2$Cl with H$_2$NNMe$_2$ (eq 5). Similar metathesis attempts with

(20) (a) Tonks, I. A.; Henling, L. M.; Day, M. W.; Bercaw, J. E. *Inorg. Chem.* **2009**, *48*, 5096. (b) Agapie, T.; Bercaw, J. E. *Organometallics* **2007**, *26*, 2957–2959. (c) Agapie, T.; Day, M. W.; Bercaw, J. E. *Organometallics* **2008**, *27*, 6123–6142. (d) Agapie, T.; Henling, L. H.; DiPasquale, A. G.; Rheingold, A. L.; Bercaw, J. E. *Organometallics* **2008**, *27*, 6245–6246. (e) Golisz, S. R.; Bercaw, J. E. *Macromolecules* **2009**, *42*, 8751.

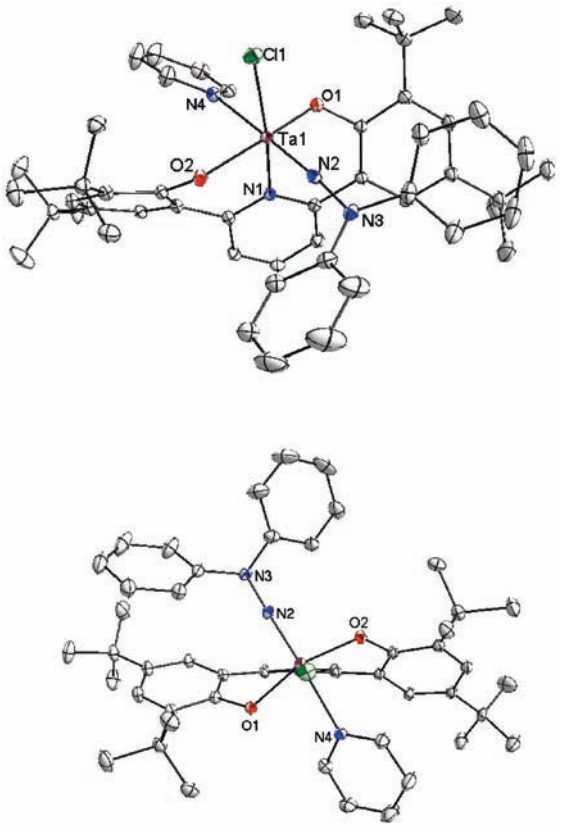


**Figure 4.** Thermal ellipsoid drawing of **8**. Side view and view the Cl−Ta bond showing $C_2$-symmetric arrangement of the (ONO) ligand. Selected bond lengths (Å) and angles (deg): Ta1−O1 1.9762(8); Ta1−O2 1.9856(7); Ta1−N1 2.246(1); Ta1−N2 1.7925(8); Ta1−N4 2.3598(8); N2−N3 1.355(1); Ta1−N2−N3 174.62(8). H atoms removed for clarity.

H$_2$NNPh$_2$ yielded no reaction, likely because of the increased steric bulk of diphenylhydrazine versus dimethylhydrazine. We have previously reported that sterically bulky primary amines (e.g., $^t$BuNH$_2$) do not react with (ONO)Ta(NMe$_2$)$_2$Cl or (ONO)TaMe$_3$, whereas less bulky amines such as aniline do react to form imides.[20a]

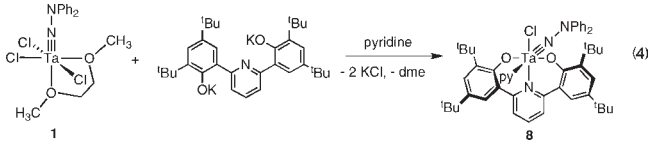


(4)

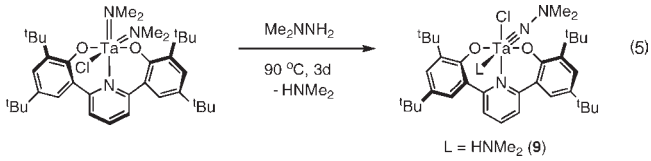


(5)

Both **8** and **9** have been characterized by X-ray diffraction. The former contains a meridionally bound *bis*(phenolate) ligand with the diphenylhydrazide ligand *trans* to an additional molecule of pyridine (Figure 4). Similar to complex **1**, the hydrazido-(2-) ligand forms an LX$_2$ triple bond with tantalum, evidenced from the Ta−N bond length of 1.7925(8) Å and an essentially linear Ta−$N_\alpha$−$N_\beta$ angle of 174.62(8)°. The $N_\alpha$−$N_\beta$ bond distance of 1.355(1) Å is again shorter than that in free diphenylhydrazine because of reduced $N_\alpha$−$N_\beta$ lone pair repulsion.

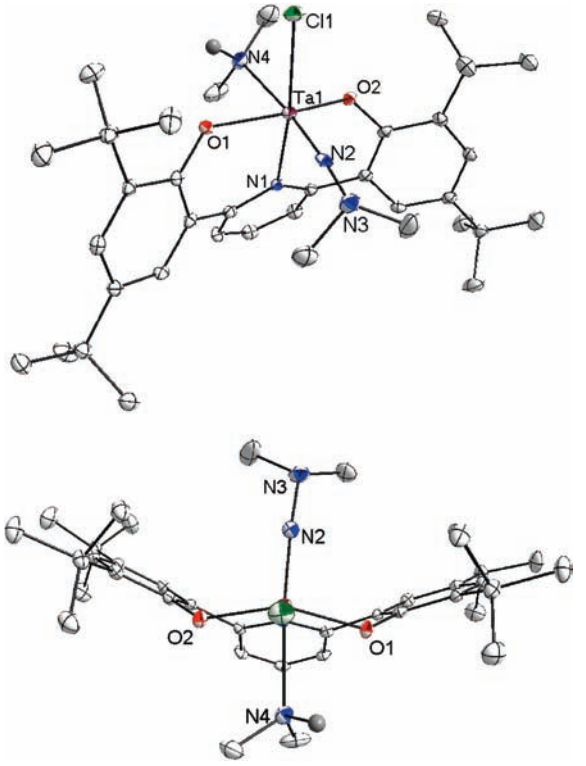


**Figure 5.** Thermal ellipsoid drawing of **9**. Side view and view down the Cl−T bond showing $C_S$-symmetric arrangement of the (ONO) ligand. Selected bond lengths (Å) and angles (deg): Ta1−O1 1.970(1); Ta1−O2 1.968(1); Ta1−N1 2.303(1); Ta1−N2 1.789(1); Ta1−N4 2.443(1); N2−N3 1.356(2); Ta1−N2−N3 175.2(1). H atoms (except for H on the N4 amine) removed for clarity.

Similar to **8**, **9** contains a meridionally bound *bis*(phenolate) ligand with the dimethylhydrazido(2-) ligand *trans* to the weakest *trans* influencing ligand $HNMe_2$ (Figure 5). The short Ta−N distance of 1.789(1) Å and linear $Ta-N_\alpha-N_\beta$ angle of 175.2(1)° once again indicate a Ta−N triple bond for the [Ta≡N−$NMe_2$] moiety. Complex **9** is the only dimethylhydrazido(2-) complex that we have fully characterized and provides a valuable structural contrast to **8**, which contains the same basic (ONO)TaLX(NR) framework. For **9** the (ONO) ligand is bound in a $C_S$-symmetric fashion, whereas in **8** the ligand geometry is $C_2$-symmetric. Given the close similarity of the two complexes, we can only suggest that the smaller methyl substituents of the dimethylhydrazido (2-) complex **9** are able to accommodate the electronically preferred[20a] $C_s$-symmetric arrangement of (ONO), as is also found in the corresponding phenyl imido derivative (ONO)-Ta($HNMe_2$)Cl(≡NPh).[20a] The structure of **8** suggests that the larger $N_\beta$-phenyl groups would clash with the bulky *tert*-butyl groups on the *bis*(phenolate) ligand such that the (ONO) ligand twists to accommodate the less sterically hindered $C_2$-symmetric (ONO) geometry for the diphenylhydrazido complex. The geometry about $N_\beta$ also generates greater steric crowding for the diphenylhydrazido (2-) complex **8**: while the $Ta-N_\alpha$ and $N_\alpha-N_\beta$ bonding metrics are roughly the same in **8** and **9**, the geometry about $N_\beta$ is different in the two complexes. In **8** (as in **1**, and other diphenylhydrazido complexes), $N_\beta$ is almost planar with bond angles of approximately 117° for $N_\alpha-N_\beta-C_{ipso}$ and 123° for $C_{ipso}-N_\beta-C_{ipso}$. In contrast, **9** $N_\beta$ is pyramidal with all angles near 111°. This geometry change could also influence the overall ligand geometry.

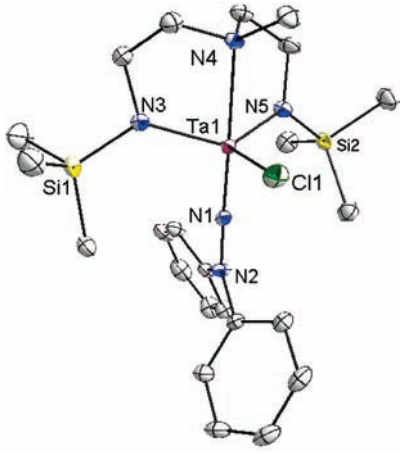


**Figure 6.** Thermal ellipsoid drawing of **10**. Selected bond lengths (Å) and angles (deg): Ta1−N1 1.7988(1); Ta1−N3 2.0197(1); Ta1−N4 2.3815(1); Ta1−N5 2.0113(1); N1−N2 1.363(1); Ta1−N1−N2 177.42. H atoms removed for clarity.

Mountford,[5b,c,e] Odom,[6] and Gade[7] have utilized tridentate, dianionic *bis*(amido)amine/pyridine ligand sets to explore the structure and reactivity of group 4 hydrazido(2-) complexes. These compounds can act as catalysts for hydrohydrazination reactions or as catalysts for a unique alkyne *bis*-amination reaction. We sought to make analogous cationic group 5 complexes, envisioning that the increased Lewis acidity of a cationic Ta center would promote reactivity.

Reaction of **1** with $MeN[(CH_2)_2NTMS)]_2Li_2$ in benzene produces the *bis*(amide)amine complex, ($C_2-N_2N^{Me}$)TaCl($NNPh_2$) (**10**), in high yield (eq 6). The $^1$H NMR spectrum for **10** shows that the ($C_2-N_2N^{Me}$) ligand is bound *fac* to Ta, as 4 non-equivalent protons for the methylenes of the backbone of the ligand are observed as multiplets. Similar reaction of **1** with the propylene backbone ligand, $MeN[(CH_2)_3NTMS)]_2Li_2$, also produces the desired complex ($C_3-N_2N^{Me}$)TaCl($NNPh_2$) (**11**), albeit in lower yield (eq 7). The methylene backbone protons for **11** are much broader than in **10**, suggesting that the structure is fluxional at room temperature. Despite the ill-defined methylenes, **11** can be easily identified in the $^1$H NMR from the characteristic $NNPh_2$ resonances, the N-Me resonance, and the slightly broadened $SiMe_3$ resonance.

Large orange crystals of **10** were grown by slow diffusion of a concentrated hexane solution of **10** into $TMS_2O$. Complex **10** is monomeric, 5-coordinate trigonal bipyramidal with the ($C_2-N_2N^{Me}$) ligand bound in *fac*- manner as predicted by $^1$H NMR (Figure 6). The diphenyhydrazido ligand, which is *trans* to the tertiary amine of the ($C_2-N_2N^{Me}$) ligand, has a Ta−N bond length of 1.7988(1) Å and a $Ta-N_\alpha-N_\beta$ bond angle of 177.4(1)°, consistent with the metrics of an $LX_2$ Ta−N triple bond as is the case for the other hydrazido complexes reported here.

Perhaps the most notable feature of **10** is the position of the hydrazido ligand relative to the ($C_2-N_2N^{Me}$) ligand. In the Mountford[5b,e] group 4 analogues, the diphenylhydrazido ligand is located in the equatorial plane of the trigonal bipyramid, whereas in **10** it lies in an axial position. From an orbital overlap perspective, the *trans* isomer observed in **10** would seem to be favored because the hydrazide and the two amides would then not compete for the same metal

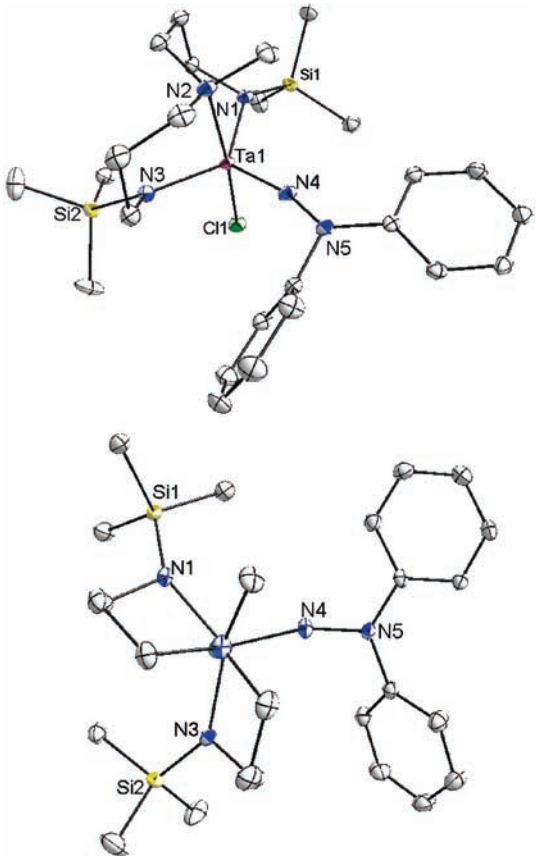


**Figure 7.** Thermal ellipsoid drawing of **11**. Side view and top-down view showing *cis*-fused decalin-type metallacycle structure. Selected bond lengths (Å) and angles (deg): Ta1−N1 2.004(1); Ta1−N2 2.328(1); Ta1−N3 2.006(1); Ta1−N4 1.791(1); N4−N5 1.374(2); Ta1−N4−N5 163.75(9). H atoms removed for clarity.

d $\pi$ orbitals. Additionally, the strong *trans* influencing imido should prefer to be opposite the very weakly *trans* influencing tertiary amine. Because all of Mountford's imido and hydrazido complexes have a *cis* conformation, this structure might well require further investigation.

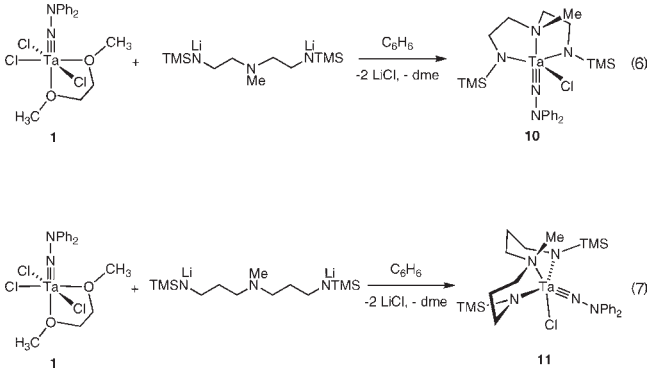


**11** was crystallized by diffusion of pentane into a concentrated solution of **11** in $CH_2Cl_2$. **11** is a $C_1$-symmetric molecule with a *fac*-coordinated ($C_3$−$N_2N^{Me}$) ligand that resembles a *cis*-fused decalin bicyclic ring structure (Figure 7). Unlike **10** and similar to the complexes observed by Mountford and Gade, **11** contains a diphenylhydrazido ligand roughly *cis* to the amine in the ($C_3$−$N_2N^{Me}$) ligand. The Ta−N distance of 1.791(1) Å is consistent with triple bond, although the Ta−$N_\alpha$−$N_\beta$ bond angle (163.75(9)°) is

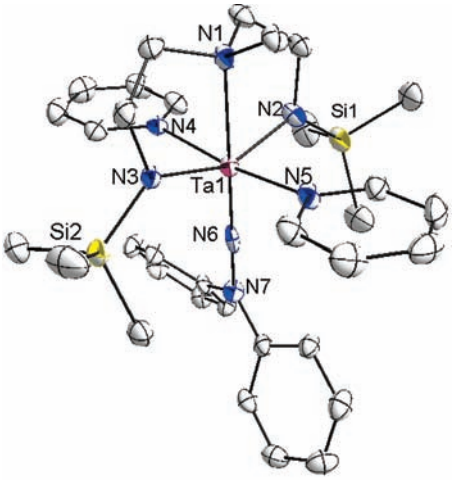


**Figure 8.** Thermal ellipsoid drawing of **13**. Selected bond lengths (Å) and angles (deg): Ta1−N1 2.379(3); Ta1−N2 2.055(3); Ta1−N3 2.047(3); Ta1−N4 2.314(4); Ta1−N5 2.280(4); Ta1−N6 1.762(3); N6−N7 1.402(4); Ta1−N6−N7 177.6(3). H atoms and $BArF_{24}$ counteranion removed for clarity.

**Scheme 2**

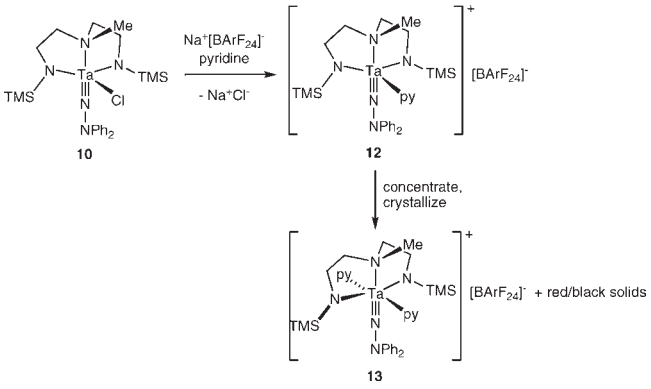


significantly bent compared to other Ta−$NNPh_2$ complexes. This bending could be caused by steric repulsion from one of the $SiMe_3$ groups also located in the equatorial plane. When complex **10** was treated with $Na^+[BArF_{24}]^-$ ($[BArF_{24}]^-$ = $[B(3,5\text{-}(CF_3)_2C_6H_3)_4]^-$) in $CH_2Cl_2$ in the presence of excess pyridine, the cationic chloride-abstracted product [($C_2$−$N_2N^{Me}$)Ta($NNPh_2$)(py)][$BArF_{24}$] (**12**) was generated with concomitant precipitation of NaCl (Scheme 2). Without the presence of pyridine, or in the presence of a weaker ligand such as 2,6-lutidine, $PPh_3$, or perfluoropyridine, reaction with $NaBArF_{24}$ led to fast decomposition after chloride abstraction. Complex **12** has been identified by $^1$HNMR and $^{13}$CNMR and is consistent with the coordination of one molecule of pyridine to a cationic ($C_2$−$N_2N^{Me}$)Ta($NNPh_2$) fragment with $[BArF_{24}]^-$ as the counteranion.

Attempts to carry out pyridine substitution reactions with a variety of ligands (e.g., 4-*tert*-butyl pyridine, $PPh_3$, THF), as well as attempted and [2 + 2] reactions with terminal and internal alkynes resulted in no reaction. The inertness of **12** was unexpected, particularly considering that it is isoelectronic with analogous neutral, group 4 imido complexes. Attempts to crystallize **12** have instead yielded the *bis*-(pyridine) adduct, [($C_2$−$N_2N^{Me}$)Ta($NNPh_2$)($py)_2$][$BArF_{24}$] (**13**), along with significant amounts of intractable noncrystalline solids (Scheme 2). Addition of 1 equiv of pyridine in

the reaction of **10** with $NaBArF_{24}$ yields 100% conversion to **12** ($^1$H NMR), so we are confident that **12** is the major product upon chloride abstraction rather than the crystallographically observed **13**. Additionally, elemental analysis of **12** is consistent with a *mono*(pyridine) rather than a *bis*(pyridine) adduct. Similar reaction with 4-$^t$Bu-pyridine gives an adduct with a 9:18 integration ratio of $^t$Bu:$SiMe_3$ peaks in the $^1$H NMR, consistent with a product analogous to **12**. As a result of this evidence, **13** is rather a decomposition product of **12**.

Complex **13** contains a meridionally bound ($C_2-N_2N^{Me}$) ligand with the diphenylhydrazido moiety *trans* to the amine of the ($C_2-N_2N^{Me}$) ligand and the two coordinated pyridine molecules mutually *trans* (Figure 8). The Ta−N $LX_2$ triple bond distance is 1.762(3), slightly shorter than in **10** as would be expected for a tantalum cation, and the $Ta-N_\alpha-N_\beta$ bond angle is 177.6(3)°.

## Conclusions

The complexes $(dme)MCl_3(NNPh_2)$ (M = Ta, **1**; Nb, 2) have been prepared from $MCl_5$ and diphenylhydrazine via a Lewis-acid assisted dehydrohalogenation reaction. Complex **1** is blue whereas related imidos are colorless or yellow. This color arises from an LMCT from a Ta-hydrazide $\pi$-bonding HOMO that is destabilized because of an antibonding interaction with the lone pair of the hydrazido $N_\beta$. Complex **1** has been shown to be a versatile synthon for installing a $[Ta{=}NNPh_2]$ moiety into a variety of inorganic or organometallic coordination complexes with other neutral, mono- or dianionic ligand sets. The bonding metrics of all of the reported $[Ta{=}NNR_2]$ complexes are consistent with $LX_2$-type Ta−N triple bonds based on short Ta−N distances and mostly linear $Ta-N_\alpha-N_\beta$ bond angles. In an attempt to generate cationic Ta analogues of reported group 4 hydrazido complexes, a chloride abstraction for **10** was performed with $Na^+[BArF_{24}]^-$ to yield a pyridine adduct, cation, **12**, which is surprisingly inert to ligand substitution and [2 + 2] reactions with alkynes. We are currently further exploring the reactivity of the tantalum-hydrazido moiety as it relates to that for the analogous tantalum-imido complexes.

## Experimental Section

**General Considerations and Instrumentation.** All air- and moisture-sensitive compounds were manipulated using standard high vacuum and Schlenk techniques or manipulated in a glovebox under a nitrogen atmosphere. Solvents for air- and moisture-sensitive reactions were dried over sodium benzophenone ketyl and stored over titanocene where compatible or dried by the method of Grubbs.[21] Pyridine was dried over sodium and distilled prior to use. $TaCl_5$ was purchased from Strem Chemicals and was sublimed prior to use. Diphenylhydrazine and dimethylhydrazine were purchased from TCI and were distilled from $CaH_2$ and degassed prior to use. All other materials were used as received. $Na^+[BArF_{24}]^-$,[22] NaCp,[23] and (2,6-$(OC_6H_2$-$^t$$Bu_2)_2C_5H_3N)K_2$[20d] were prepared following literature procedures. Benzene-$d_6$ was purchased from Cambridge Isotopes and dried over sodium benzophenone ketyl, while methylene chloride-$d_2$, also purchased from Cambridge Isotopes, was dried over $CaH_2$ and filtered through a plug of activated alumina. $^1$H and $^{13}$C spectra were recorded on Varian Mercury 300 or Varian INOVA 500 spectrometers, and chemical shifts are reported with respect to residual protio-solvent impurity for $^1$H (s, 7.16 ppm for $C_6D_5H$; t, 5.32 ppm for $CDHCl_2$) and solvent carbons for $^{13}$C (t, 128.39 for $C_6H_6$; p, 54.00 for $CD_2Cl_2$). It was difficult to obtain satisfactory CHN combustion analysis for some of the compounds prepared. For these compounds, spectroscopic data is available in the Supporting Information.

**Computational Details.** Density functional calculations were carried out using Gaussian 03 Revision D.01.[24] Calculations were performed using the nonlocal exchange correction by Becke[25,26] and nonlocal correlation corrections by Perdew,[27] as implemented using the b3lyp[28,29] keyword in Gaussian. The following basis sets were used: LANL2DZ[30−32] for Ta atoms and 6-31G** basis set for all other atoms. Pseudopotentials were utilized for Ta atoms using the LANL2DZ ECP. All optimized structures were verified using frequency calculations and did not contain any imaginary frequencies. Isosurface plots were made using the Gaussian 03 Revision D.01 program.[24]

**X-ray Crystal Data: General Procedure.** Crystals were removed quickly from a scintillation vial to a microscope slide coated with Paratone N oil. Samples were selected and mounted on a glass fiber with Paratone N oil. Data collection was carried out on a Bruker KAPPA APEX II diffractometer with a 0.71073 Å MoK$\alpha$ source. The structures were solved by direct methods. All non-hydrogen atoms were refined anisotropically. Some details regarding refined data and cell parameters are available in Tables 1 and 2.

**Synthesis of ($\kappa^2$-$CH_3O(CH_2)_2OCH_3$)$TaCl_3(NNPh_2)$ (1).** $TaCl_5$ (500 mg, 1.4 mmol) and $ZnCl_2$ (380 mg, 2.8 mmol) were mixed in 10 mL of $CH_2Cl_2$ in an inert atmosphere glovebox. Dimethoxyethane (0.25 mL) was added to the reaction mixture, and the reaction stirred for 15 min, yielding a dark solution with a white precipitate. The reaction was cooled to −30 °C and 1,1-diphenylhydrazine (230 $\mu$L, 258 mg, 1.4 mmol) and pyridine (226 $\mu$L, 221 mg, 2.8 mmol) in 5 mL of $CH_2Cl_2$ was slowly added to the reaction mixture. The initially orange solution slowly turned deep blue and was left to stir overnight. The reaction was then filtered to remove pyridinium-zinc chloride salts, $CH_2Cl_2$ was removed in vacuo, and the resulting blue solid was washed with pentane and then was dissolved into 20 mL of benzene, filtered, and lyophilized to yield 700 mg of **1** as a blue powder (90%). Further purification was achieved by crystallization

(21) Pangborn, A. B.; Giardello, M. A.; Grubbs, R. H.; Rosen, R. K.; Timmers, F. J. *Organometallics* **1996**, *15*, 1518.
(22) Brookhart, M.; Grant, B.; Volpe, A. F., Jr. *Organometallics* **1992**, *11*, 3920.
(23) Panda, T. K.; Gamer, M. T.; Roesky, P. W. *Organometallics* **2003**, *22*, 877–878.
(24) Frisch, M. J.; Trucks, G. W.; Schlegel, H. B.; Scuseria, G. E.; Robb, M. A.; Cheeseman, J. R.; Montgomery, Jr., J. A.; Vreven, T.; Kudin, K. N.; Burant, J. C.; Millam, J. M.; Iyengar, S. S.; Tomasi, J.; Barone, V.; Mennucci, B.; Cossi, M.; Scalmani, G.; Rega, N.; Petersson, G. A.; Nakatsuji, H.; Hada, M.; Ehara, M.; Toyota, K.; Fukuda, R.; Hasegawa, J.; Ishida, M.; Nakajima, T.; Honda, Y.; Kitao, O.; Nakai, H.; Klene, M.; Li, X.; Knox, J. E.; Hratchian, H. P.; Cross, J. B.; Bakken, V.; Adamo, C.; Jaramillo, J.; Gomperts, R.; Stratmann, R. E.; Yazyev, O.; Austin, A. J.; Cammi, R.; Pomelli, C.; Ochterski, J. W.; Ayala, P. Y.; Morokuma, K.; Voth, G. A.; Salvador, P.; Dannenberg, J. J.; Zakrzewski, V. G.; Dapprich, S.; Daniels, A. D.; Strain, M. C.; Farkas, O.; Malick, D. K.; Rabuck, A. D.; Raghavachari, K.; Foresman, J. B.; Ortiz, J. V.; Cui, Q.; Baboul, A. G.; Clifford, S.; Cioslowski, J.; Stefanov, B. B.; Liu, G.; Liashenko, A.; Piskorz, P.; Komaromi, I.; Martin, R. L.; Fox, D. J.; Keith, T.; Al-Laham, M. A.; Peng, C. Y.; Nanayakkara, A.; Challacombe, M.; Gill, P. M. W.; Johnson, B.; Chen, W.; Wong, M. W.; Gonzalez, C.; Pople, J. A. *Gaussian 03*, revision C.02; Gaussian, Inc.: Wallingford, CT, 2004.
(25) Becke, A. D. *Phys. Rev. A: At., Mol., Opt. Phys.* **1988**, *38*, 3098–3100.
(26) Becke, A. D. *J. Chem. Phys.* **1988**, *88*, 1053–1062.
(27) Perdew, J. P. *Phys. Rev. B* **1986**, *33*, 8800–8802.
(28) Lee, C.; Yang, W.; Parr, R. G. *Phys. Rev. B* **1988**, *37*, 785.
(29) Miehlich, B.; Savin, A.; Stoll, H.; Preuss, H. *Chem. Phys. Lett.* **1989**, *157*, 200.
(30) Hay, P. J.; Wadt, W. R. *J. Chem. Phys.* **1985**, *82*, 270–283.
(31) Wadt, W. R.; Hay, P. J. *J. Chem. Phys.* **1985**, *82*, 284–298.
(32) Hay, P. J.; Wadt, W. R. *J. Chem. Phys.* **1985**, *82*, 299–310.

**Table 1.** Crystal and Refinement Data for Complexes **1**, **7**, **8**, and **9**

| | **1** | **7** | **8** | **9** |
|---|---|---|---|---|
| empirical formula | $C_{16}H_{20}N_2O_2Cl_3Ta$ | $C_{22}H_{20}N_2ClTa$ | $C_{50}H_{58}N_4O_2ClTa$ | $C_{37}H_{56}N_4O_2ClTa$ |
| formula weight | 559.64 | 528.80 | 963.40 | 805.26 |
| $T$ (K) | 100(2) | 100(2) | 100(2) | 100(2) |
| $a$, Å | 13.4839(6) | 19.1261(8) | 15.6102(8) | 34.7022(12) |
| $b$, Å | 10.2768(4) | 10.2503(4) | 20.2128(10) | 9.2582(3) |
| $c$, Å | 14.8254(7) | 19.2383(8) | 15.7963(8) | 23.1835(9) |
| α, deg | | | | |
| $\beta$, deg | 108.079(2) | 100.720(2) | 113.066(3) | |
| $\gamma$, deg | | | | |
| volume, Å$^3$ | 1952.95(15) | 3705.8(3) | 4585.7(4) | 7448.4(5) |
| $Z$ | 4 | 8 | 4 | 8 |
| crystal system | monoclinic | monoclinic | monoclinic | orthorhombic |
| space group | $P2_1/c$ | $P2_1/n$ | $P2_1/c$ | $Pbcn$ |
| $d_{calc}$, g/cm$^3$ | 1.903 | 1.896 | 1.395 | 1.436 |
| $\theta$ range, deg | 1.59 to 52.22 | 2.26 to 40.86 | 1.73 to 40.11 | 1.76 to 36.42 |
| $\mu$, mm$^{-1}$ | 6.049 | 6.084 | 2.498 | 3.059 |
| abs. correction | semi emp. | semi emp. | semi emp. | none |
| GOF | 1.388 | 1.495 | 1.718 | 1.939 |
| $R_1$, [a] $wR_2$ [b] [$I > 2\sigma(I)$] | 0.0285, 0.0362 | 0.0271, 0.0400 | 0.0250, 0.0380 | 0.0401, 0.0439 |

[a] $R_1 = \sum||F_o| - |F_c||/\sum|F_o|$. [b] $wR_2 = [\sum w(F_o^2 - F_c^2)^2/\sum w(F_o^2)^2]^{1/2}$.

**Table 2.** Crystal and Refinement Data for Complexes **10**, **11**, and **13**

| | **10** | **11** | **13** |
|---|---|---|---|
| empirical formula | $C_{23}H_{39}N_5Si_2ClTa$ | $C_{25}H_{43}N_5Si_2ClTa$ | $[C_{33}H_{49}N_7Si_2Ta]^+[C_{32}H_{12}BF_{24}]^-$ |
| formula weight | 658.17 | 686.22 | 1644.15 |
| $T$ (K) | 100(2) | 98(2) | 100(2) |
| $a$, Å | 13.1052(6) | 8.1959(4) | 22.0650(16) |
| $b$, Å | 12.9574(6) | 10.4496(5) | 13.9417(10) |
| $c$, Å | 16.9529(8) | 34.5115(14) | 24.4542(16) |
| α, deg | | | |
| $\beta$, deg | 90.622(3) | 94.059(2) | 114.312(4) |
| $\gamma$, deg | | | |
| volume, Å$^3$ | 2878.6(2) | 2948.3(2) | 6855.6(8) |
| $Z$ | 4 | 4 | 4 |
| crystal system | monoclinic | monoclinic | monoclinic |
| space group | $P2_1/n$ | $P2_1/n$ | $P2_1/n$ |
| $d_{calc}$, g/cm$^3$ | 1.519 | 1.546 | 1.593 |
| $\theta$ range, deg | 1.95 to 43.76 | 2.04 to 38.82 | 1.62 to 27.70 |
| $\mu$, mm$^{-1}$ | 4.014 | 3.922 | 1.750 |
| abs. correction | semi emp. | semi emp. | semi emp. |
| GOF | 2.205 | 1.754 | 1.652 |
| $R_1$, [a] $wR_2$ [b] [$I > 2\sigma(I)$] | 0.0285, 0.0506 | 0.0235, 0.0341 | 0.0387, 0.0666 |

[a] $R_1 = \sum||F_o| - |F_c||/\sum|F_o|$. [b] $wR_2 = [\sum w(F_o^2 - F_c^2)^2/\sum w(F_o^2)^2]^{1/2}$.

through vapor diffusion of pentane into a concentrated dichloroethane solution of **1**, yielding **1** as blue/royal blue dichroic needles. $^1$HNMR (300 MHz, $CD_2Cl_2$) $\delta$, ppm: 3.985 (s, 3H, OC$H_3$); 4.023 (s, 3H, OC$H_3$); 4.136 (m, 2H, OC$H_2$); 4.152 (m, 2H, OC$H_2$); 7.05 (m, 2H, aryl); 7.425 (m, 8H, aryl). $^{13}$CNMR (125 MHz, $CD_2Cl_2$) $\delta$, ppm: 63.71, 70.91, 72.31, 76.45 ($CH_3OCH_2CH_2OCH_3$); 105.33, 120.86, 125.05, 129.35 (aryl). Calcd for $C_{16}H_{20}Cl_3N_2O_2Ta$: C 34.34, H 3.60, N 5.01; Found: C 34.57, H 3.66, N 4.99%.

**Synthesis of ($\kappa^2$-$CH_3O(CH_2)_2OCH_3$)$NbCl_3$($NNPh_2$) (2).** $NbCl_5$ (160 mg, 0.6 mmol) and $ZnCl_2$ (162 mg, 1.2 mmol) were mixed in 10 mL of $CH_2Cl_2$ in an inert atmosphere glovebox. Dimethoxyethane (0.2 mL) was added to the reaction mixture and stirred for 15 min, yielding a dark solution with a yellowish precipitate. The reaction was cooled to −30 °C, and 1,1-diphenylhydrazine (110 mg, 0.6 mmol) and pyridine (94 mg, 96 $\mu$L, 1.2 mmol) in 2 mL of $CH_2Cl_2$ were slowly added to the reaction mixture. The mixture turned dark blue/green, and was left to stir overnight, during which period it turned dark green with a white precipitate. The reaction was then filtered, and $CH_2Cl_2$ removed in vacuo. The resulting green residue was washed with pentane, then dissolved into 10 mL of benzene, filtered, and then lyophilized to yield **2** as 220 mg (78%) of a dull green powder. $^1$HNMR (300 MHz, $CD_2Cl_2$) $\delta$, ppm: 3.840 (s, 3H, OC$H_3$); 3.944 (s, 3H, OC$H_3$); 4.089 (s, 4H, OC$H_2$); 7.166 (m, 2H, aryl); 7.454 (m, 8H, aryl). $^{13}$CNMR (125 MHz, $CD_2Cl_2$) $\delta$, ppm: 63.22, 69.68, 72.08, 76.01 ($CH_3OCH_2CH_2OCH_3$); 120.90, 126.10, 129.70, 143.03 (aryl).

**Synthesis of (py)$_2$$TaCl_3$($NNPh_2$) (3). 1** (72 mg, 0.13 mmol) was dissolved in 1 mL of neat pyridine and stirred overnight. The reaction quickly turned very dark green/blue. After 16 h, the reaction was filtered and solvent removed in vacuo to give **3** quantitatively as a dark teal solid. $^1$HNMR (500 MHz, $CD_2Cl_2$) $\delta$, ppm: 7.02 (m, 2H, aryl); 7.35 (m, 8H, aryl); 7.48 (m, 6H, pyridyl); 7.86 (t, 1H, pyridyl); 7.95 (t, 1H, pyridyl); 8.64 (d, 2H, pyridyl); 9.07 (d, 2H, pyridyl). $^{13}$CNMR (125 MHz, $CD_2Cl_2$) $\delta$, ppm: 121.09, 124.87, 125.17, 125.46, 129.23, 139.85, 140.58, 143.17, 152.42, 152.75 (aryl).

**Synthesis of (tmeda)$TaCl_3$($NNPh_2$) (4). 1** (60 mg, 0.1 mmol) was dissolved in 1 mL of neat TMEDA. The reaction turned dark blue and was stirred overnight. The reaction mixture was filtered and solvent removed in vacuo to give **4** as a dark blue solid (52 mg, 90%). $^1$HNMR (500 MHz, $CD_2Cl_2$) $\delta$, ppm: 2.571 (s, 12H, N(C$H_3$)$_2$); 2.705 (s, 4H, NC$H_2$); 6.604 (m, 2H, aryl); 7.254 (m, 8H, aryl). $^{13}$CNMR (125 MHz, $CD_2Cl_2$) $\delta$, ppm: 48.08 (N$CH_3$); 57.37 (N$CH_2$); 118.14, 121.27, 124.88, 143.78 (aryl).

**Synthesis of (bpy)$TaCl_3$($NNPh_2$) (5). 1** (28 mg, 0.05 mmol, 1eq) in 2 mL of $C_6H_6$ was added to solid 2,2′-bipyridine (78 mg, 0.5 mmol, 10 equiv) and stirred overnight. The reaction slowly turned green. After 16 h, the reaction was filtered, solvent removed in vacuo, and the remaining green residue was washed successively with 35 mL portions of pentane to give **5** as a green solid. $^1$HNMR (300 MHz, $CD_2Cl_2$) $\delta$, ppm: 7.04(t, 2H, aryl); 7.39 (m, 4H, aryl); 7.50 (t, 1H, bpy); 7.58 (d, 4H, aryl); 7.90 (t, 1H, bpy); 8.23 (m, 2H, bpy); 8.31 (m, 2H, bpy); 9.08 (d, 1H, bpy); 9.69 (d, 1H, bpy).

**Synthesis of (THF)$_2$$TaCl_3$($NNPh_2$) (6). 1** (20 mg, 0.036 mmol) was dissolved in 2 mL of THF and stirred for 20 min. The reaction mixture turned from blue to purple, and solvent was removed in vacuo to yield **6** and some decomposition products. **6** is not stable in solution which precludes its pure isolation, but can quickly be characterized by $^1$HNMR. $^1$HNMR (300 MHz, $CD_2Cl_2$) $\delta$, ppm: 1.95 (br, 8H, C$H_2CH_2O$); 4.20 (br, 8H, $CH_2CH_2O$); 7.02 (m, 2H, aryl); 7.39 (m, 8H, aryl).

**Synthesis of $Cp_2TaCl$($NNPh_2$) (7).** Solid **1** (91 mg, 0.163 mmol) and NaCp (28.4 mg, 0.326 mmol) were placed in a 50 mL round-bottom flask fitted with a needle valve and

evacuated on a high vacuum line. A 20 mL portion of tetrahydrofuran (THF) was distilled onto the mixture at −78 °C, then the reaction mixture was warmed to room temperature and stirred overnight. Afterward, the reaction mixture was filtered, solvent removed in vacuo, and the resulting red residue was extracted into 20 mL of toluene. Removal of the toluene in vacuo yielded 60 mg (70% yield) of **7** as an orange/red solid. Further purification could be obtained by layering pentane onto a concentrated, −30 °C solution of **7** in toluene which gave high yields of orange, X-ray quality crystals of **7** upon cooling the system to −30 °C. $^1$HNMR (300 MHz, $CD_2Cl_2$) $\delta$, ppm: 5.990 (s, 10H, $C_5H_5$); 7.064 (m, 2H, aryl); 7.356 (m, 8H, aryl). $^{13}$CNMR (125 MHz, $C_6D_6$) $\delta$, ppm: 110.09 ($C_5H_5$); 121.47, 124.36, 129.67, 145.46 (aryl).

**Synthesis of (2,6-(OC$_6$H$_2$-$^t$Bu$_2$)$_2$C$_5$H$_3$N)TaCl(NNPh$_2$)(py) (8).** (ONO)H$_2$ (194.5 mg, 0.4 mmol) was deprotonated with KBn (104.2 mg, 0.8 mmol) in 10 mL of $C_6H_6$ over the course of 2 h in an inert atmosphere glovebox. After 2 h, (dme)$TaCl_3(NNPh_2)$ (244 mg, 0.4 mmol) and pyridine (31.6 mg, 0.4 mmol) in 10 mL of $C_6H_6$ were added to the reaction mixture. The reaction was stirred for 24 h, filtered, and solvent removed in vacuo. The resulting orange residue was washed with pentane, yielding **8** as 350 mg (91%) of a yellow/orange solid. Yellow/orange crystals suitable for X-ray diffraction were obtained through pentane vapor diffusion into a concentrated $CH_2Cl_2$ solution. $^1$HNMR (300 MHz, $CD_2Cl_2$) $\delta$, ppm: 1.28 (s, 18H, C(C$H_3$)$_3$); 1.42 (s, 18H, C(C$H_3$)$_3$); 6.87 (m, 8H, aryl); 7.03 (m, 4H, aryl); 7.20 (s, 2H, aryl); 7.38 (s, 2H, aryl) 7.49 (t, 1H, pyridyl); 7.69 (d, 2H, pyridyl); 7.91 (t, 1H, pyridyl); 8.30 (d, 2H, pyridyl). $^{13}$CNMR (125 MHz, $C_6D_6$) $\delta$, ppm: 30.40 (C($C$H$_3$)$_3$); 31.91 (C($C$H$_3$)$_3$); 34.66 ($C$(CH$_3$)$_3$); 35.58 ($C$(CH$_3$)$_3$); 120.12, 122.96, 123.69, 124.10, 124.63, 125.80, 126.79, 128.85, 136.85, 138.53, 138.86, 141.39, 145.21, 150.53, 155.55, 159.17 (aryl).

**Synthesis of (2,6-(OC$_6$H$_2$-$^t$Bu$_2$)$_2$C$_5$H$_3$N)TaCl(NNMe$_2$)(HNMe$_2$) (9).** A 10 mL Schlenk tube fitted with a Teflon needle valve was charged with (ONO)Ta(NMe$_2$)$_2$Cl (106 mg, 0.135 mmol), $H_2NNMe_2$ (8.08 mg, 10.2 $\mu$L, 0.135 mmol), a stirbar, and 5 mL of $C_6H_6$ in an inert atmosphere glovebox. The vessel was sealed and placed in an oilbath preheated to 90 °C and left to stir for 3 days, where it turned orange/red. After 3 days, the solvent and $HNMe_2$ were removed in vacuo, and the yellow-orange residue was washed with 20 mL of hexanes to yield 50 mg of **9** as a yellow-orange powder (43%). $^1$HNMR (300 MHz, $CD_2Cl_2$) $\delta$, ppm: 1.344 (s, 18H, C(C$H_3$)$_3$); 1.489 (s, 18H, C(C$H_3$)$_3$); 1.905 (br s, 6H, HN(C$H_3$)$_2$); 2.082 (s, 6H, NN(C$H_3$)$_2$); 2.433 (m, 1H, $H$NMe$_2$); 7.358 (d, 2H, aryl); 7.497 (d, 2H, aryl); 7.758 (d, 2H, pyridyl); 8.009 (t, 1H, pyridyl). $^{13}$CNMR (125 MHz, $C_6D_6$) $\delta$, ppm: 30.48 (C($C$H$_3$)$_3$); 31.94 (C($C$H$_3$)$_3$); 34.84 ($C$Me$_3$); 35.66 ($C$Me$_3$); 38.57 (HN($C$H$_3$)$_2$); 47.97 (NN($C$H$_3$)$_2$); 124.33, 124.91, 126.42, 127.02, 128.85, 137.41, 141.95, 157.94, 158.92 (aryl).

**Synthesis of ($\kappa^3$-MeN[(CH$_2$)$_2$NTMS)]$_2$)TaCl(NNPh$_2$) (10).** MeN[(CH$_2$)$_2$NTMS)]$_2$Li$_2$ (418 mg, 1.53 mmol) and (dme)$TaCl_3(NNPh_2)$ (856 mg, 1.53 mmol) were mixed in 20 mL of $C_6H_6$ in an inert atmosphere glovebox. The reaction quickly turned from dark blue to deep orange, and was left to stir overnight. The reaction was filtered and the benzene lyophilized off, and the orange residue was extracted into 60 mL of pentane. The pentane was removed in vacuo to yield 720 mg (71%) of **10** as a sticky orange solid. Cystals suitable for X-ray diffraction were grown from vapor diffusion out of a concentrated hexanes solution into $TMS_2O$. $^1$HNMR (500 MHz, $CD_2Cl_2$) $\delta$, ppm: 0.03 (s, 18H, NSi(C$H_3$)$_3$); 2.76 (s, 3H, NC$H_3$); 2.79 (m, 2H −C$H$HCH$_2$−); 3.15 (m, 2H −CH$H$CH$_2$−); 3.83 (m, 2H, −CH$_2$C$H$H−); 3.91 (m, 2H, −CH$_2$CH$H$−); 6.90 (t, 2H, aryl); 7.26 (m, 4H, aryl); 7.45 (d, 4H, aryl). $^{13}$CNMR (125 MHz, $C_6D_6$) $\delta$, ppm: 1.834 (Si($C$H$_3$)$_3$); 45.87 (N$C$H$_3$); 49.59 (N$C$H$_2$CH$_2$); 57.54 (N$C$H$_2$CH$_2$); 119.83, 122.19, 128.84, 144.10. Calcd for $C_{23}H_{39}ClN_5Si_2Ta$: C 41.97, H 5.97, N 10.64; Found: C 42.49, H 6.43, N 9.99%.

**Synthesis of ($\kappa^3$-MeN[(CH$_2$)$_3$NTMS)]$_2$)TaCl(NNPh$_2$) (11).** MeN[(CH$_2$)$_3$NTMS)]$_2$Li$_2$ (94.3 mg, 0.313 mmol) and (dme)$TaCl_3(NNPh_2)$ (175 mg, 0.313 mmol) were mixed in 10 mL of $C_6H_6$ in an inert atmosphere glovebox. The reaction quickly turned from dark blue to deep orange/red, and was left to stir overnight. The reaction was filtered and solvent removed in vacuo, and the resulting orange residue was washed with pentane. **11** was crystallized by vapor diffusion of pentane into a concentrated solution of **11** in $CH_2Cl_2$, yielding 40% as orange/red crystals. $^1$HNMR (300 MHz, $CD_2Cl_2$) $\delta$, ppm: 0.172 (br s, 18H, NSi(C$H_3$)$_3$); 1.654 (br m, 4H, −CH$_2$C$H_2$-CH$_2$−); 2.853 (s, 3H, NC$H_3$); 3.446 (br m, 8H, −C$H_2$CH$_2$-C$H_2$−); 6.962 (m, 2H, aryl); 7.315 (m, 8H, aryl). $^{13}$CNMR (125 MHz, $C_6D_6$) $\delta$, ppm: 1.07 (Si($C$H$_3$)$_3$); 27.85 (−$C$H$_2$−); 53.18 (N$C$H$_3$); 120.70, 123.37, 129.27, 146.29 (aryl). Calcd for $C_{25}H_{43}ClN_5Si_2Ta$: C 43.76, H 6.32, N 10.21; Found: C 42.50, H 6.49, N 9.99%.

**Synthesis of [($\kappa^3$-MeN[(CH$_2$)$_2$NTMS)]$_2$)Ta(py)(NNPh$_2$)][B(3,5-(CF$_3$)$_2$C$_6$H$_3$)$_4$] (12). 10** (160 mg, 0.243 mmol) and pyridine (19.2 mg, 19.6 $\mu$L, 0.243 mmol) were premixed in an inert atmosphere glovebox in 4 mL of $CH_2Cl_2$. The solution of **10** and pyridine was then added to solid $Na^+[BArF_{24}]^-$ (215.5 mg, 0.243 mmol). The reaction mixture quickly turned from yellow to orange as the $Na^+[BArF_{24}]^-$ went into solution. The reaction mixture was stirred for 30 min; then the solvent was removed in vacuo. The dark orange residue was washed with pentane, yielding 346 mg **12** (91%) as a dark orange/red solid. $^1$HNMR (500 MHz, $CD_2Cl_2$) $\delta$, ppm: 0.207 (s, 18H, Si(C$H_3$)$_3$); 2.035 (s, 3H, NC$H_3$); 2.712 (m, 4H, NC$H_2$CH$_2$); 4.124 (m, 2H, NC$H$-HCH$_2$); 4.256 (m, 2H, NC$H$HCH$_2$); 6.281 (d, 4H, $o$-C$_6$H$_5$); 6.801 (t, 2H, $p$-C$_6$H$_5$); 6.871 (m, 4H $m$-C$_6$H$_5$); 7.570 (s, 4H, $p$-C$_6$H$_3$(CF$_3$)$_2$); 7.738 (s, 8H, $o$-C$_6$H$_3$(CF$_3$)$_2$); 8.205 (t, 1H, pyridyl); 8.831 (d, 2H, pyridyl); 8.950 (br, 2H, pyridyl). $^{13}$CNMR (125 MHz, $C_6D_6$) $\delta$, ppm: Calcd for $C_{60}H_{56}BF_{24}N_6Si_2Ta$: C 46.05, H 3.61, N 5.37; Found: C 46.22, H 3.56, N 5.44%.

**Acknowledgment.** We thank Dr. Nilay Hazari (Yale) for assistance with the DFT calculations. DFT calculations were carried out using the Molecular Graphics and Computation Facility, College of Chemistry, University of California, Berkeley, CA, with equipment support from NSF Grant CHE-0233882. We acknowledge Dr. Jay Labinger and Professor Harry Gray (Caltech) and Professor Lisa McElwee-White (University of Florida) for fruitful discussions. We also thank Lawrence Henling and Dr. Michael Day for assistance with the X-ray studies. The Bruker KAPPA APEXII X-ray diffractometer was purchased via an NSF CRIF:MU award to the California Institute of Technology, CHE-0639094. This work has been supported by USDOE Office of Basic Energy Sciences (Grant DE-FG03-85ER13431).

**Supporting Information Available:** Tables of bond lengths, angles, and anisotropic displacement parameters for the presented solid-state structures. X-ray crystallographic data files (CIF) of compounds **1**, **7**, **8**, **9**, **10**, **11**, and **13**. NMR spectra for compounds with unsatisfactory CHN combustion analysis. This material is available free of charge via the Internet at http://pubs.acs.org. The crystallographic data for compounds **1** (CCDC 719414), **7** (CCDC 767430), **8** (CCDC 719322), **9** (CCDC 754732), **10** (CCDC 719036), **11** (CCDC 752439), and **13** (CCDC 739782) have been deposited with the Cambridge Crystallographic Data Center and can be obtained by requesting the deposition numbers.